

Metal enrichment via ram pressure stripping in the IGM of the compact galaxy group RGH 80 *

Hai-Juan Cui¹, Hai-Guang Xu¹, Jun-Hua Gu¹, Jing-Ying Wang¹, Li-Yi Gu¹, Yu Wang¹, Zhen-Zhen Qin¹ and Tao An²

¹ Department of Physics, Shanghai Jiao Tong University, Shanghai 200240, China;
hgxu@sjtu.edu.cn

² Shanghai Astronomical Observatory, Chinese Academy of Sciences, Shanghai 200030, China

Received 2009 November 2; accepted 2009 December 29

Abstract By creating and analyzing two dimensional gas temperature and abundance maps of the RGH 80 compact galaxy group with high-quality *Chandra* data, we detect a high-abundance ($\simeq 0.7 Z_{\odot}$) arc, where the metal abundance is significantly higher than the surrounding regions by $\simeq 0.3 Z_{\odot}$. This structure shows tight spatial correlations with the member galaxy PGC 046529, as well as with the arm-like feature identified on the X-ray image in the previous work of Randall et al. (2009). Since no apparent signature of AGN activity is found to be associated with PGC 046529 in multi-band observations, and the gas temperature, metallicity, and mass of the high-abundance arc resemble those of the ISM of typical early-type galaxies, we conclude that this high-abundance structure is the remnant of the ISM of PGC 046529, which was stripped out of the galaxy by ram pressure stripping due to the motion of PGC 046529 in RGH 80. This novel case shows that ram pressure stripping can work as efficiently in the metal enrichment process in galaxy groups as it can in galaxy clusters.

Key words: galaxies: clusters: individual (RGH 80) — galaxy: abundance — intergalactic medium — X-rays: galaxies: clusters

1 INTRODUCTION

In galaxy groups and clusters, the intergalactic medium (IGM) is enriched with the metals synthesized in the stellar interior, which were released into the vast intergalactic space mainly via mergers (e.g., Durret et al. 2005), galactic wind (e.g., Nath & Trentham 1997), and AGN activities (e.g., Simionescu et al. 2009). As of today, the details of how these mechanisms work and how effective they are at different evolution stages of the IGM are still unclear (e.g., Aguirre et al. 2001; Hayakawa et al. 2004, 2006). Although AGN feedback has been regarded as the most popular and effective process to enrich the IGM, the work of, e.g., Hayakawa et al. (2004, 2006) still showed that the ram pressure stripping caused by mergers may have played a crucial role in removing metals from galaxies.

* Supported by the National Natural Science Foundation of China.

Very few cases of ram pressure stripping of metal-enriched gas contained in galaxies have been reported in literature (e.g., Sun et al. 2007; Hayakawa et al. 2004, 2006), and all these cases were found in galaxy clusters, where the dynamical environment is complicated. However, in compact galaxy groups where there exist much fewer member galaxies as compared with the clusters, the galaxy number density is actually as high as that of the core region of a rich cluster, so that strong interactions between member galaxies are often observed (e.g., Carlberg et al. 1994). This indicates that compact galaxy groups are ideal sites for us to study the effects of ram pressure stripping of metal-enriched gas held in the member galaxies.

The compact galaxy group RGH 80 ($z = 0.0377$) may be such an ideal place. In 2009, Randall et al. reported that there exist interactions between the dominant galaxy PGC 046515 (E, Vorontsov-Velyaminov et al. 2001; R.A. = $13^{\text{h}}20^{\text{m}}14.8^{\text{s}}$, Dec = $+33^{\text{d}}08^{\text{m}}37.7^{\text{s}}$, J2000, Brinkmann et al. 2000) and the member galaxy PGC 046529 (E, Vorontsov-Velyaminov et al. 2001; R.A. = $13^{\text{h}}20^{\text{m}}17.8^{\text{s}}$, Dec = $+33^{\text{d}}08^{\text{m}}41.2^{\text{s}}$, J2000, Rines et al. 2003), and ascribed the origin of an arm-like X-ray feature identified on the X-ray map to the ram pressure stripping. However, a detailed analysis of the two dimensional distribution of gas metallicity, which is of fundamental importance for studying the origin of the X-ray arm, was not provided by the authors.

In this work, we calculate and study the two dimensional spatial distributions of both gas temperature and abundance of the hot IGM of RGH 80 with the high-quality *Chandra* data archived at the *Chandra* X-ray Observatory Science Center that is operated by the Smithsonian Astrophysical Observatory. We find firm evidence that the IGM of this group is being enriched via the ram pressure stripping caused by the motion of the member galaxy PGC 046529. Throughout the paper, we quote errors at a 90% confidence level unless mentioned otherwise. We adopt the solar abundance standard of Grevesse & Sauval (1998), where the iron abundance relative to hydrogen is 3.16×10^{-5} in number, and employ the cosmological parameters $H_0 = 71 h_{71} \text{ km s}^{-1} \text{ Mpc}^{-1}$, $\Omega_m = 0.27$, $\Omega_\Lambda = 0.73$, so that $1''$ corresponds to $44.2 h_{71}^{-1} \text{ kpc}$.

2 OBSERVATIONS AND DATA REDUCTION

The RGH 80 group was observed with *Chandra* on 2005 November 1 (ObsID 6941) for a total exposure of 39.1 ks with CCDs 2, 3, 5, 6, and 7 of the Advanced CCD Imaging Spectrometer (ACIS) in operation. The center of the group-dominating galaxy PGC 046515 was positioned close to the nominal point on the back-illuminated S3 chip (CCD 7) with a small offset of $0.18'$. The events were collected with a frame time of 3.2 s and telemetried in the VFaint mode, as the focal plane temperature was set to -120° . In this work, we use the standard *Chandra* data analysis package CIAO software (version 3.4.0) and apply the latest CALDB (version 4.1.1) to process the data extracted from the ACIS-S3 chip. We keep events with *ASCA* grades 0, 2, 3, 4 and 6, and remove all the bad pixels, bad columns, columns adjacent to bad columns and node boundaries. We examine the lightcurves extracted from the source-free regions on the S3 chip and detect no strong occasional background flares. Based on the above processings, we obtain a total of about 1.2×10^5 photons in the level-2 S3 event list.

3 X-RAY AND OPTICAL IMAGES

In Figure 1(a) and (b) we show the $0.7 - 7 \text{ keV}$ *Chandra* ACIS-S3 image that has been corrected for exposure and smoothed with a Gaussian kernel of $4''$, and the corresponding Digitized Sky Survey (DSS) B-band image of RGH 80, respectively. We find that the position of the X-ray peak (R.A. = $13^{\text{h}}20^{\text{m}}14.7^{\text{s}}$, Dec = $+33^{\text{d}}08^{\text{m}}36.3^{\text{s}}$) is consistent with the optical center of the galaxy PGC 046515 within about $2.3''$, while another major member galaxy PGC 046529 is located $0.64'$ east of PGC 046515. The distribution of the diffuse X-ray emission is roughly symmetric within the central $\simeq 0.5'$ ($22.1 h_{71}^{-1} \text{ kpc}$). Outside the central region, we confirm the result of Randall et al. (2009) that there exists an arm-like X-ray feature in the northeast direction, which spans from north

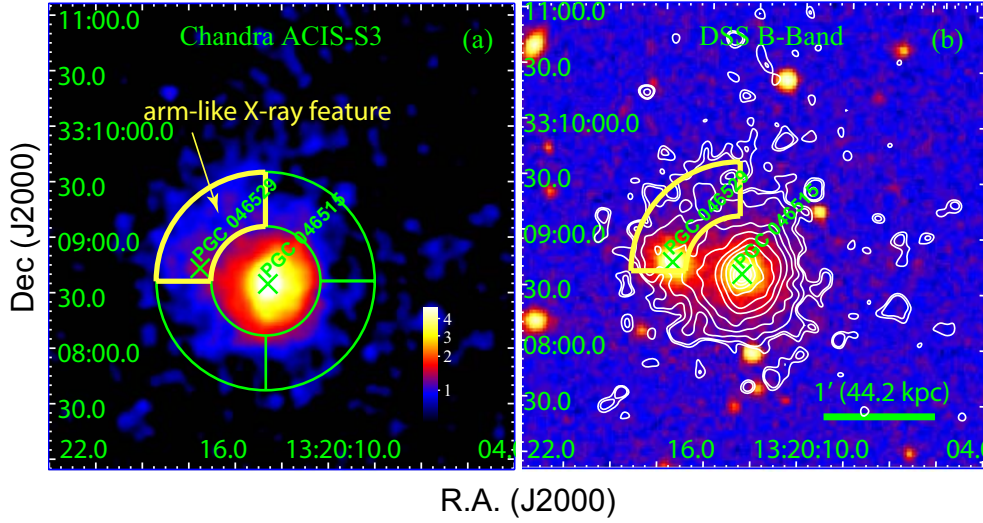


Fig. 1 (a) 0.7 – 7 keV *Chandra* ACIS-S3 image that has been corrected for exposure and smoothed with a Gaussian kernel of $4''$. The unit of the color bar is $10^{-8} \text{ cts s}^{-1} \text{ cm}^{-2} \text{ pixel}^{-2}$. The four pie regions are used to extract and compare the surface brightness of the arm-like feature with other directions. (b) The DSS B-band optical image of RGH 80 overlaid with the X-ray intensity contours calculated from (a), with the contours ranging from $7 \times 10^{-9} \text{ cts s}^{-1} \text{ cm}^{-2} \text{ pixel}^{-2}$ to $6 \times 10^{-8} \text{ cts s}^{-1} \text{ cm}^{-2} \text{ pixel}^{-2}$. In both (a) and (b), we mark the positions of PGC 046515 and PGC 046529 with two crosses and the arm-like X-ray feature with the yellow pie region (see also fig. 1 in Randall et al. 2009).

to east with one of its ends connected to PGC 046529 (Fig. 1(a)). To quantitate the significance of this feature, we calculate the averaged 0.7 – 7 keV surface brightness of the four pie regions, which are defined in Figure 1(a), with the northeast one covering the arm-like feature. We find that the averaged surface brightness of the northeast pie region is $5.1 \pm 0.2 \times 10^{-9} \text{ cts s}^{-1} \text{ cm}^{-2} \text{ pixel}^{-2}$, which is significantly higher than those of other pie regions ($3.2 \pm 0.1 \times 10^{-9} \text{ cts s}^{-1} \text{ cm}^{-2} \text{ pixel}^{-2}$, $3.1 \pm 0.1 \times 10^{-9} \text{ cts s}^{-1} \text{ cm}^{-2} \text{ pixel}^{-2}$, and $3.2 \pm 0.1 \times 10^{-9} \text{ cts s}^{-1} \text{ cm}^{-2} \text{ pixel}^{-2}$ for the southeast, southwest, and northwest pie regions, respectively) at the 90% confidence level. The appearance of this arm-like feature implies the existence of strong distortion in this region. Using the group's average temperature $\simeq 1 \text{ keV}$ (Xue et al. 2004), we calculate the local sound speed to be $\simeq 400 \text{ km s}^{-1}$, which means that the sound crossing time over the width $\simeq 0.3' (13.3 h_{71}^{-1} \text{ kpc})$ of this feature is $\simeq 30 \text{ Myr}$, a time that can be regarded as an approximation to the upper limit of the feature's lifetime.

4 2-D SPECTRAL ANALYSIS

Following the method of Gu et al. (2007), we calculate the two dimensional temperature and abundance maps of the X-ray gas and their corresponding 1σ error maps (Fig. 2). At the first step, we distribute a set of 1000 sampling knots on the sky plane, with the surface density distribution of the sampling knots proportional to the X-ray surface brightness distribution. Next, we divide the group with the CVT cells (Diehl & Statler 2006) generated around these sampling knots. We extract the spectrum from a circular region centered on each sampling knot, which encloses more than 1000 photons in 0.7 – 7 keV (including the background) after all the identified point sources are excluded.

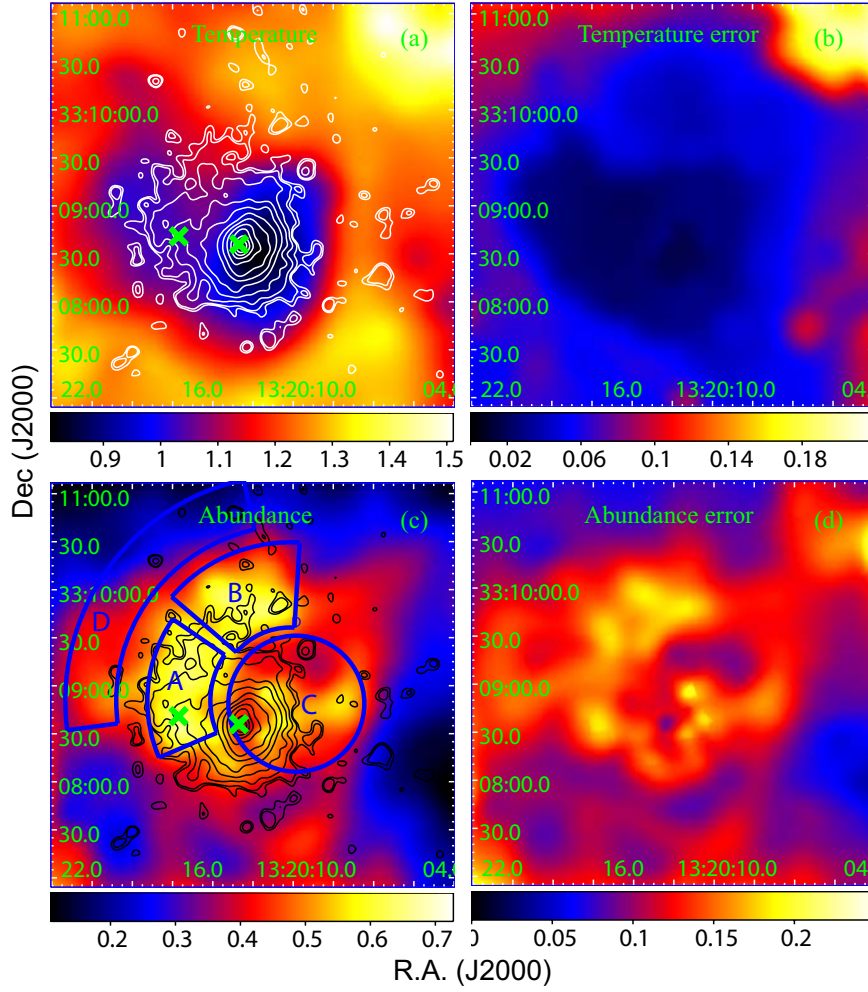


Fig. 2 (a) The temperature map of RGH 80 overlaid with the X-ray contours (Fig. 1(b)). (b) The 1σ error map for the temperature distribution. (c) The abundance map of RGH 80 overlaid with the X-ray contours (Fig. 1(b)). Regions A, B, C, and D are used to extract the spectra to confirm the existence of the high-abundance arc. (d) The 1σ error map for the abundance distribution. In both (a) and (c), we mark the position of PGC 046515 and PGC 046529 with two crosses.

The extracted spectrum is fitted with an absorbed APEC model (XSPEC v.12.4.0), with the absorption fixed to the Galactic column density $N_{\text{H}} = 1.05 \times 10^{20} \text{ cm}^{-2}$ (Dickey & Lockman 1990), and the redshift fixed to 0.0377. The *Chandra* blank field spectra are used as the background. We assign the obtained temperature and abundance to the corresponding CVT cell, and repeat this process for all the sampling knots. Finally, we obtain the temperature and abundance maps through adaptively smoothing the tessellated images with a Gaussian kernel, whose scale is set to be the radii of the CVT cells. Error maps are created in a similar way.

We find that both the temperature and abundance distributions appear to be highly asymmetric. Figure 2(a) shows that the center cool ($< 1 \text{ keV}$) region shows an apparent offset from the X-ray peak to the west, which agrees with the distortions illustrated on the X-ray image (Fig. 1(a)). To the

east of the X-ray peak, there is a relatively low temperature ($\simeq 1$ keV) region, which encloses the member galaxy PGC 046529. On the abundance map, we identify an impressive high-abundance arc that spans from north to east, with a radius of $\simeq 1.24'$ ($54.9 h_{71}^{-1}$ kpc) and a width of $\simeq 0.8'$ ($35.4 h_{71}^{-1}$ kpc). The abundances in and around the arc are $\simeq 0.7 \pm 0.1 Z_{\odot}$ and $0.4 \pm 0.1 Z_{\odot}$ (68% confidence level), respectively.

In order to verify the reliability of our detection of the high-abundance arc, we extract the spectra from regions A and B that are defined on the arc, and regions C and D that are defined outside the arc (Fig. 2(c)). The spectra are fitted with an absorbed APEC model (Fig. 3), with the absorption again fixed to the galactic value $N_{\text{H}} = 1.05 \times 10^{20} \text{ cm}^{-2}$ (Dickey & Lockman 1990), and the redshift fixed to 0.0377. We summarize the best-fit results in Table 1, which appear to be consistent with those implied in the temperature and abundance maps (Fig. 2). By studying the two-dimensional fit-statistic contours of gas temperature and metal abundance at the 68% and 90% confidence levels for regions A, B, C, and D (Fig. 4), we are confident that the metal abundance in the arc region is higher than those of the neighboring regions at a significance of 90%. The existence of the high-abundance arc is hence confirmed.

In order to compare the high-abundance structure with the spatial distributions of X-ray emission and star lights, in Figure 2(c) we overlay the X-ray surface brightness contours on the abundance map, and mark the locations of the central galaxy PGC 046515 and member galaxy PGC 046529 with two crosses. We find that the arm-like X-ray feature (Sect. 3) perfectly coincides with the high-abundance arc, and the member galaxy PGC 046529 is located right at one end of the high-abundance arc or the arm-like feature. These spatial correlations indicate that both the arm-like X-ray feature and high-abundance arc may be connected with PGC 046529.

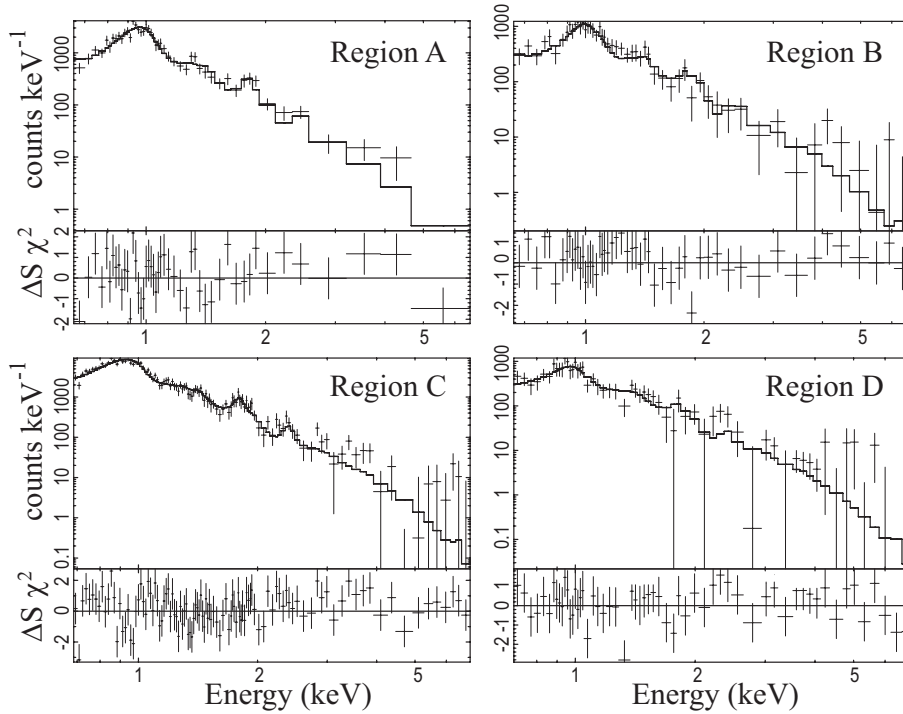


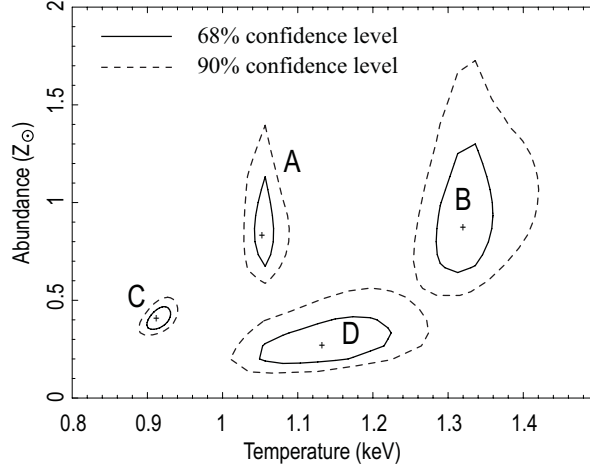
Fig. 3 Spectra extracted from the four regions defined in Fig. 2(c) and the best-fit models (see also Table 1).

Table 1 Best-fit Spectral Models for the Four Regions Defined in Fig. 2(c)[†]

Region No.	Temperature (keV)	Abundance (Z_{\odot})	χ^2/dof
A	1.05 ± 0.03	$0.83^{+0.57}_{-0.24}$	49.4/45
B	$1.32^{+0.09}_{-0.07}$	$0.87^{+0.85}_{-0.35}$	38.07/49
C	$0.92^{+0.02}_{-0.03}$	$0.40^{+0.10}_{-0.08}$	121.02/106
D	$1.14^{+0.14}_{-0.12}$	$0.27^{+0.13}_{-0.10}$ [‡]	64.98/56

[†] We fit the spectra with an absorbed APEC model with the absorption and redshift fixed to the Galactic value ($N_{\text{H}} = 1.05 \times 10^{20} \text{ cm}^{-2}$; Dickey & Lockman 1990) and $z = 0.0377$.

[‡] The confidence level is 68% for the abundance of region D.

**Fig. 4** Two-dimensional fit-statistic contours of temperature and abundance at the 68% and 90% confidence levels for the four regions defined in Fig. 2(c).

5 DISCUSSION

We detect a high-abundance arc in the RGH 80 compact group, which shows tight spatial correlations with both the arm-like X-ray feature and the member galaxy PGC 046529. A reasonable and natural way to explain these correlations is to assume that the excess emission in the arm-like X-ray feature is due to the excess iron contained in the high-abundance arc, which originated from PGC 046529. However, can this be real? First, we note that the gas temperature (1.1 – 1.3 keV) and abundance ($\simeq 0.7 Z_{\odot}$) of the high-abundance arc fall into the temperature and abundance range of early-type galaxies. On the other hand, considering that the metal abundance in the arc is about $0.3 Z_{\odot}$ higher than its surrounding regions, and using the gas density profile given in Xue et al. (2004), we estimate that the total gas mass of the arm-like feature is $M_{\text{gas}} \simeq 5.4 \pm 0.5 \times 10^{10} M_{\odot}$, so that the excess iron mass therein is $M_{\text{Fe}} \simeq 4.7^{+6.5}_{-0.7} \times 10^6 M_{\odot}$. Assuming the time dependent type Ia supernova rate in Dahlen et al. (2004) and the wind mass loss rate in Ciotti et al. (1991), these amounts of gas and iron are close to the lower limit of gas and iron mass of the inter-stellar medium (ISM) of early-type galaxies, and can easily be produced in PGC 046529 within only $\simeq 0.4$ Gyr, which strongly supports the idea that the high-abundance gas was originally contained in PGC 046529. Since there are no signatures of AGN activity (e.g., X-ray cavity and radio substructures) in PGC 046529, the possibility of the asymmetric high-abundance arc being formed by AGN activity can be excluded.

immediately. Hence, the ram pressure stripping due to the motion of PGC 046529 becomes the most likely mechanism.

By examining Figure 2, we also note that the gas temperature in the high-abundance arc varies from $\simeq 1.3$ keV in the north (region B) to $\simeq 1.1$ keV in the east (region A). Using the best-fit spectral parameters from region A that are presented in Table 1 and equation (6) of Gu et al. (2009), we estimate that the time needed for the low temperature gas stripped out of PGC 046529 to achieve a thermal equilibrium with the surrounding IGM via thermal conduction is $t_{\text{cond}} \simeq 0.2$ Gyr. On the other hand, based on the velocity dispersion (450 km s^{-1} ; Ramella et al. 2002) of this group, we roughly estimate that the time needed for PGC 046529 to travel a distance equal to the separation between region B and region A is $t_{\text{B} \rightarrow \text{A}} \simeq 0.15$ Gyr. Since $t_{\text{cond}} \simeq t_{\text{B} \rightarrow \text{A}}$ and PGC 046529 is located in region A, the spatial variation of gas temperature from region B to region A strongly supports the idea that the high abundance gas was stripped out of PGC 046529, and has been conductively heated since then.

Compared with the two straight gas tails behind the infalling galaxy ESO 137–001 in Abell 3627, as found by Sun et al. (2009), the spatial distribution of the high-abundance gas in RGH 80 forms a curved shape around PGC 046529, and possesses a width much wider than the gas tails behind ESO 137–001. This could be ascribed to the low spatial resolution ($\simeq 0.8'$ on the high-abundance arc) of our abundance map. Besides, since the location of PGC 046529 from the group center ($30.5 h_{71}^{-1} \text{ kpc}$) is significantly less than the Roche limit

$$d \simeq 2.44 \left(\frac{M}{\frac{4}{3}\pi\rho_m} \right)^{1/3} \simeq 182 h_{71}^{-1} \text{ kpc}, \quad (1)$$

where $\rho_m \simeq 5 \times 10^{-26} \text{ g cm}^{-3}$ is the density of the gas stripped from PGC 046529, and $M \simeq 1.5 \times 10^{12} M_{\odot}$ is the total gravitational mass contained inside the radius of PGC 046529 (Xue et al. 2004), it is possible that the high-abundance arc has also been significantly broadened by the tidal force. Such an off-center enrichment process may help explain the central metal abundance dip observed in many galaxy clusters and groups (e.g., Abell 3266, Henriksen & Tittley 2002; the NGC 1550 group, Sun et al. 2003).

Based on the above analysis and discussion, we conclude that the high-abundance gas around the member galaxy PGC 046529 in RGH 80 is a remnant of the ISM of this galaxy, which was blown outwards by the ram pressure due to the motion of PGC 046529. This novel case shows that the ram pressure can serve as an efficient metal enrichment mechanism in galaxy groups, just as in galaxy clusters.

6 SUMMARY

With the high-quality *Chandra* ACIS data, we detect a high-abundance arc structure, in which the metal abundance is significantly higher than the surrounding regions by $\simeq 0.3 Z_{\odot}$. This structure shows tight spatial correlations with member galaxy PGC 046529, as well as with the arm-like feature identified on the X-ray image in the previous work of Randall et al. (2009). Since no AGN activity is found in PGC 046529, and the gas temperature, metallicity and mass resemble those of the ISM of early-type galaxies, we conclude that the high-abundance arc is the remnant of the ISM of PGC 046529, which was efficiently stripped out of this galaxy by ram pressure.

Acknowledgements We thank the *Chandra* team for making data available via the High Energy Astrophysics Science Archive Research Center (HEASARC) at <http://heasarc.gsfc.nasa.gov>. This work was supported by the National Natural Science Foundation of China (Grant Nos. 10673008, 10878001 and 10973010), the Ministry of Science and Technology of China (Grant No. 2009CB824900/2009CB24904), and the Ministry of Education of China (the NCET Program).

References

- Aguirre, A., Hernquist, L., Schaye, J., Katz, N., Weinberg, D. H., & Gardner, J. 2001, *ApJ*, 561, 521
- Brinkmann, W., Laurent-Muehleisen, S. A., Voges, W., et al. 2000, *A&A*, 356, 445
- Carlberg, R. G., Pritchet, C. J., & Infante, L. 1994, *ApJ*, 435, 540
- Ciotti, L., D’Ercole, A., Pellegrini, S., & Renzini, A. 1991, *ApJ*, 376, 380
- Dahlen, T., et al. 2004, *ApJ*, 613, 189
- Dickey, J. M., & Lockman, F. J. 1990, *ARA&A*, 28, 215
- Diehl, S., & Statler, T. S. 2006, *MNRAS*, 368, 497
- Durret, F., Lima Neto, G. B., & Forman, W. 2005, *Advances in Space Research*, 36, 618
- Grevesse, N., & Sauval, A. J. 1998, *Space Science Reviews*, 85, 161
- Gu, J., Xu, H., Gu, L., An, T., Wang, Y., Zhang, Z., & Wu, X.-P. 2007, *ApJ*, 659, 275
- Gu, L., et al. 2009, *ApJ*, 700, 1161
- Hayakawa, A., Furusho, T., Yamasaki, N. Y., Ishida, M., & Ohashi, T. 2004, *PASJ*, 56, 743
- Hayakawa, A., Hoshino, A., Ishida, M., Furusho, T., Yamasaki, N. Y., & Ohashi, T. 2006, *PASJ*, 58, 695
- Henriksen, M. J., & Tittley, E. R. 2002, *ApJ*, 577, 701
- Nath, B. B., & Trentham, N. 1997, *MNRAS*, 291, 505
- Ramella, M., Geller, M. J., Pisani, A., & da Costa, L. N. 2002, *AJ*, 123, 2976
- Randall, S. W., Jones, C., Markevitch, M., et al. 2009, *ApJ*, 700, 1404
- Rines, K., Geller, M. J., Kurtz, M. J., & Diaferio, A. 2003, *AJ*, 126, 2152
- Simionescu, A., Werner, N., Böhringer, H., et al. 2009, *A&A*, 493, 409
- Sun, M., Donahue, M., Roediger, E., et al. 2010, *ApJ*, 708, 946
- Sun, M., Donahue, M., & Voit, G. M. 2007, *ApJ*, 671, 190
- Sun, M., Forman, W., Vikhlinin, A., Hornstrup, A., Jones, C., & Murray, S. S. 2003, *ApJ*, 598, 250
- Vorontsov-Velyaminov, B. A., Noskova, R. I., & Arkhipova, V. P. 2001, *Astronomical and Astrophysical Transactions*, 20, 717
- Xue, Y.-J., Böhringer, H., & Matsushita, K. 2004, *A&A*, 420, 833